Delta-kick cooling

In this document, we explain the method of delta-kick cooling (DKC) simulation for CAL. For the basics of the BEC on an atom chip see, e.g., Ref. [2] and for the description of the CAL chip and magnetic fields see Ref. [1]. For the sake of simplicity, we consider a Z-wire trap, even though other configurations were analyzed as well[1]. The initial trap frequencies are denoted ω^i, while the delta-kick trap frequencies are ω^i_δ. The total number of atoms is N, with N_0 of them being condensed.

Thermal cloud

The thermal cloud in the initial trap is represented by a cloud of non-interacting particles of mass m distributed normally in coordinate x^i and velocity v^i components,

$$P(x^i) = \sqrt{\frac{k_B T}{2\pi m \omega_i^2}} \exp\left(-\frac{m\omega_i^2 x_i^2}{2k_B T}\right), \quad P(v^i) = \sqrt{\frac{k_B T}{2\pi m}} \exp\left(-\frac{m v_i^2}{2k_B T}\right), \tag{1}$$

no summation by i. The first probability distribution takes into account the potential energy of the particle in a harmonic trap, while the second one is the standard Maxwell-Boltzmann distribution. Anharmonicities associated with the trap are omitted at this step, because they introduce negligible energy corrections. Number of particles in the cloud below the critical temperature is fixed by [3]

$$N_{\text{cloud}} = N - N_0 = \zeta(3)\left(\frac{k_B T}{\hbar\bar{\omega}}\right)^3, \tag{2}$$

where $\zeta(x)$ is the Riemann zeta-function ($\zeta(3) \approx 1.20$), and $\bar{\omega} \equiv \sqrt[3]{\omega_1\omega_2\omega_3}$. However, for practical reasons, we considered 1000 particles in our simulations and checked that the overall results do not change with this number being increased. The interaction between the atoms is neglected due to small s-wave scattering length for the ^{87}Rb atoms in $|2,2\rangle$ state, $a_s \sim 100\, a_0$, where a_0 is the Bohr radius.

To simulate the cloud behavior, we use simple molecular dynamics algorithm. After the initial potential is turned off, each particle position and velocity is updated by the rule

$$v_i(t+\Delta t) = v_i(t) - \frac{\nabla_i U(\vec{x}, t_i)}{m}\Delta t, \tag{3}$$

$$x_i(t+\Delta t) = x_i(t) + v_i(t)\Delta t - \frac{\nabla_i U(\vec{x}, t_i)}{m}\frac{(\Delta t)^2}{2}, \tag{4}$$

where the time-dependent potential, $U(\vec{x}, t_i) = U_\delta(\vec{x}) \exp\left(-\frac{(t-t_\delta)^2}{2\tau_\delta^2}\right)$ is defined in terms of the delta-kick potential

$$U_\delta(\vec{x}) = m_F g_F \mu_B \left(\sum_i \frac{1}{2}\partial_i^2 |B(0)| x_i^2 + \sum_{pjk} a_{pjk}\partial_p\partial_j\partial_k |B(0)| x_p x_j x_k + \cdots\right) \tag{5}$$

with quadratic part being diagonalized, moment of DKC t_δ and half-duration of DKC τ_δ. Parameter t_δ is chosen to reach desirable degree of cooling in the transverse direction x^j, $T^j_{\text{final}}/T_{\text{initial}} \sim$

[1] Z-wire creates a trap with symmetry axes co-aligned with symmetry axes of the chip. In general, this might not be true and the trap axes are defined by eigenvectors of the matrix $\partial_i\partial_j|B(\vec{x})|$

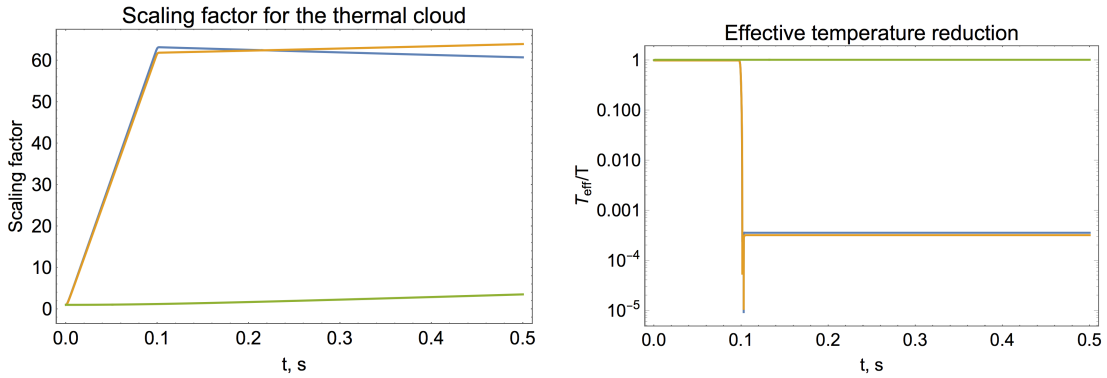

(a) (b)

Figure 1: Dynamics of the thermal cloud in a harmonic trap. (a) Scaling factors for the thermal cloud size. The lower curve corresponds to the longitudinal expansion, while the top two – to the transverse expansion.; (b) Effective temperature reduction as a result of DKC. The lower two curves correspond to the transverse directions.

$(\omega^j t_\delta)^{-2}$. Parameter τ_δ should be chosen small (typically, of order of ms) to achieve proper cancellation of particle momenta. Magnetic field is tuned such that the delta-kick stops expansion of the cloud. For an axially symmetric cloud, this condition is expressed by an approximate relation [4, 5] $\sqrt{2\pi}\tau_\delta t_\delta \omega_\delta^2 \sim 1$, i.e.,

$$\sqrt{2\pi}\, t_\delta \tau_\delta \sim \left[\frac{\mu_B m_F g_F}{m} B''(0)\right]^{-1/2}, \tag{6}$$

where derivatives are taken in the transverse direction. Practically, in order to obtain the DKC magnetic field, we rescale the Z-wire current and the bias fields of the initial trap by a single parameter A. By doing this, we make sure the initial trap and the DKC trap have the same center. One can show that, in the harmonic approximation, there always exists such A. For the sake of illustration, we present a typical result of such simulation. We start with the initial trap with frequencies $2\pi \times (100, 99, 1)$ Hz created by the chip and the thermal cloud at temperature $T = 18$ nK. The size of the cloud is given by Eq. (1): $(2.1, 2.1, 195)\mu$m. We denote the symmetry axis of this cigar-shaped cloud as the "longitudinal" direction, and the other two as the "transverse" directions. The cloud is then released from the trap and expands for $t_\delta = 100$ ms, after which the DKC applied. The DKC duration is $2\tau_\delta = 2.5$ ms and the DKC potential frequencies are $2\pi \times (10.8, 10.7, 0.1)$ Hz. This procedure results in the final effective temperatures of $(6\text{pK}, 6\text{pK}, 17\text{nK})$, i.e., cooling is achieved in the transverse directions. The effective temperatures are calculated from corresponding RMS velocities. We run the simulation to 500 ms and measure the size of the cloud, which turns out to be $(0.1, 0.1, 0.7)$ mm. We plot the relative change in the size of the cloud in Fig. 1(a) and the temperature reduction in Fig. 1(b).

If the anharmonicities are taken into account, the cubic part of the potential (5) exerts an additional vertical force on the atoms, proportional to the square of their vertical distance to the trap center. This creates a vertical gradient of temperatures with lowest temperatures T^j_{final} in the dense "core" of the cloud near to the trap center, see Fig. 3. The highest temperatures are in the sparse upper part of the cloud.

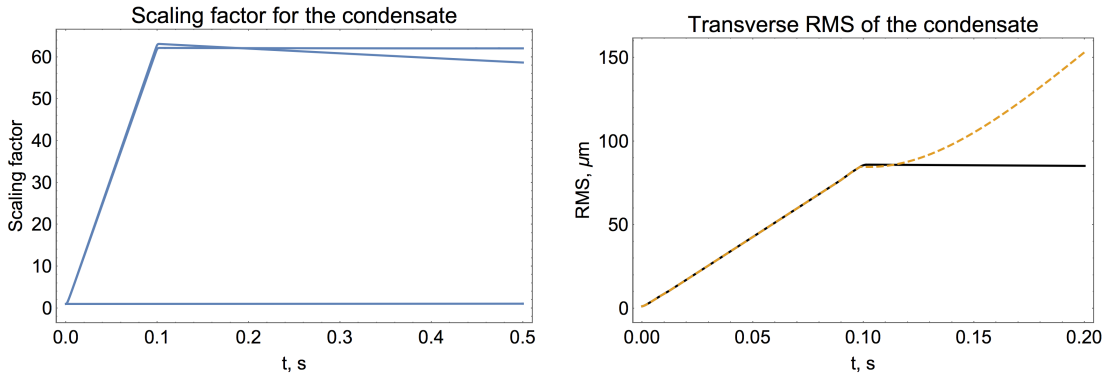

(a) (b)

Figure 2: (a) Scaling factors for condensate size in the harmonic case. The lower curve corresponds to the longitudinal expansion, while the top two – to the transverse expansion.; (b) Transverse size of the condensate in the anharmonic case. Solid line corresponds to the horizontal direction, while the dashed line corresponds to the vertical direction.

Bose-Einstein condensate

The condensate is described in terms of the complex order parameter $\Psi(\vec{x},t)$, obeying the Gross-Pitaevskii equation (GPE)

$$i\hbar\,\partial_t\Psi(\vec{x},t) = \left[-\frac{\hbar^2}{2m}\Delta + U_{ext}(\vec{x},t) + U_0|\Psi(\vec{x},t)|^2\right]\Psi(\vec{x},t)\,. \tag{7}$$

with normalization condition $\int_V d^3x|\Psi(\vec{x},t)|^2 = N_0$ and $U_0 \equiv 4\pi\hbar^2 a_s/m$. The initial state of the condensate in the trap is characterized by a time-independent version of Eq. (7) obtained by the Ansatz $\Psi(\vec{x},t) = \bar{\Psi}(\vec{x})\exp(-i\mu t/\hbar)$, where μ is the chemical potential. For a large number of condensed atoms (in our case, $N_0 \geq 1000$) one can use the standard Thomas-Fermi approximation and describe the shape of the condensate by an inverted parabola of radius [2]

$$R_i = \frac{1}{\omega_i}\sqrt{\frac{2\mu}{m}}, \qquad \mu = \frac{\hbar\bar{\omega}}{2}\left(15N_0 a_s\sqrt{\frac{m\bar{\omega}}{\hbar}}\right)^{2/5}. \tag{8}$$

In order to simulate the expansion of the condensate and the DKC we use Eq. (7) with the Thomas-Fermi initial conditions. As the first step, we choose $U_{ext}(\vec{x},t)$ to be harmonic and use the scaling solution of GPE [6] to identify approximate values of the DKC parameters. This solution is expressed in terms of scaling functions $\kappa_i(t)$ for the Fermi radii, such that $R_i(t) = \kappa_i(t)R_i(0)$ and

$$\ddot{\kappa}_i(t) = \frac{\omega_i^2}{\kappa_1(t)\kappa_2(t)\kappa_3(t)\kappa_i(t)} - \omega_{\delta,i}^2(t)\kappa_i(t), \quad \text{and } \kappa_i(0) = 1, \dot{\kappa}_i(0) = 0\,. \tag{9}$$

Typical solution is shown in Fig. 2(a). At this stage, one can see that the condensate is not expanding in the longitudinal direction, so the dynamics of the condensate in essentially "frozen" in this direction and one can perform a simplified transverse 2D simulation. At the next step, we include the cubic anharmonicities and solve Eq. (7) numerically by means of the Alternate Direction Implicit-Time Splitting pseudo Spectral (ADI-TSSP) schemes [7]. The magnetic fields of the initial trap are similar to the ones in the previous section. At this stage, the DKC parameters are being fine-tuned

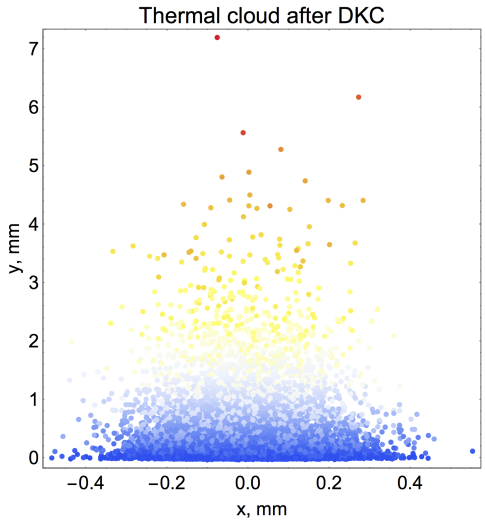

Figure 3: Side view of the thermal cloud with 10^4 particles after DKC. Horizontal direction corresponds to one of the transverse directions of the cloud, parallel to the chip surface. Vertical direction is perpendicular to the surface of the chip. The origin of coordinates is the center of the trap. Colors correspond to the logarithm of the particle's velocity, so the subclouds of the same color should be thought of as having similar order of temperature, with the lowest ones being several pK.

to ensure very slow expansion of the BEC after the delta-kick is applied, $t_\delta = 100\text{ms}, \tau_\delta = 1.5\text{ms}$. Depending on the size of the condensate, the vertical anharmonicity either stretches the condensate in the vertical direction or creates shockwaves in the condensate, further fracturing it. We show the typical results of the simulations in Fig. 4. This splitting of the condensate has no effect on the horizontal slowing down of the expansion of the condensate as a whole. However, the vertical expansion is slowed down only temporarily, see the radius-mean-squared (RMS) in Fig. 2(b). It seems that the condensate picture, Fig. 4(f), resembles the thermal cloud picture Fig. 3, where a stretched dense core is formed at the trap center.

In order to show that the condensate inhomogeneities are indeed shockwaves, we compare characteristic velocities gained by atoms in the condensate to the speed of sound.

Speed of sound

In order to calculate the speed of sound in BEC, we write down the time-dependent GPE (7) in the absence of external potential and analyze the spectrum of small excitations on top of the mean field $\bar{\Psi}(\vec{r})$,

$$\Psi(\vec{r},t) = e^{-i\mu t/\hbar}\left(\bar{\Psi}(\vec{r}) + u(\vec{r})e^{-i\omega t} + v^*(\vec{r})e^{i\omega t}\right) , \tag{10}$$

where the transformation of all quantities to the momentum space is given by

$$X(\vec{r}) = \int d^3k\, \hat{X}(\vec{k})e^{i\vec{k}\cdot\vec{r}}\,. \tag{11}$$

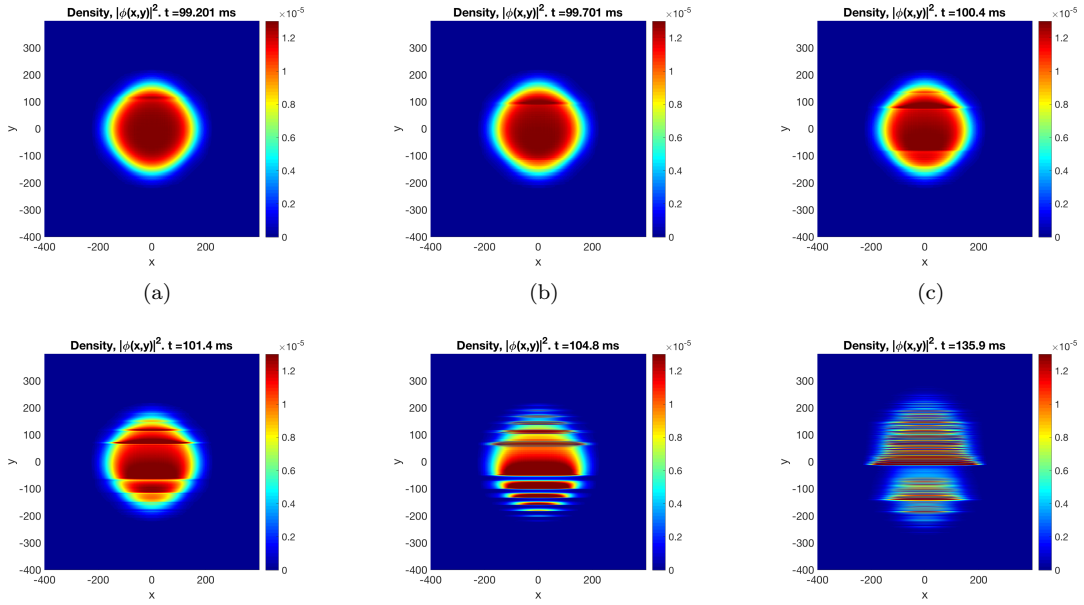

Figure 4: BEC density (a-d) during DKC; (e-f) after DKC, where the distances are measured in units $a_1 = 1.08\,\mu$m and density in units $N_0/a_1^2 = 861\,\mu\text{m}^{-2}$.

Substituting expression (10) into Eq. (7) and keeping only linear contributions in the amplitudes $u(\vec{r})$ and $v(\vec{r})$, one obtains the Bogoliubov dispersion relation [8] for the excitations,

$$\hbar\omega = \pm\sqrt{\frac{\hbar^2k^2}{2m}\left(\frac{\hbar^2k^2}{2m} + 2nU_0\right)}\,, \tag{12}$$

where we replaced the chemical potential by $\mu = nU_0$ and the particle density is $n = |\bar{\Psi}|^2$. Here the sound mode can be obtained by applying the limit $k \to 0$, leading to the linear dispersion $\omega = \pm c_s k$, where the speed of sound is

$$c_s = \sqrt{nU_0/m} = 2\hbar\sqrt{\pi n a_s}/m\,. \tag{13}$$

It is also useful to present an alternative hydrodynamic derivation of the speed of sound. Let us write Ψ in terms of density $n(\vec{x},t)$ and phase $S(\vec{x},t)$,

$$\Psi(\vec{x},t) = \sqrt{n(\vec{x},t)}\,e^{iS(\vec{x},t)/\hbar}\,. \tag{14}$$

Eq. (7) becomes

$$\partial_t\sqrt{n} = -\frac{1}{m}(\vec{\nabla}\sqrt{n})\cdot(\vec{\nabla}S) - \frac{\sqrt{n}}{2m}\Delta S\,, \tag{15}$$

$$\partial_t S = \frac{\hbar^2}{2m\sqrt{n}}\Delta\sqrt{n} - \frac{1}{2m}(\vec{\nabla}S)^2 - U_0 n\,. \tag{16}$$

By defining the velocity field as a gradient of the phase, $\vec{v} = \vec{\nabla}S/m$ one obtains coupled Madelung

equations for the phase and density of the condensate [10, 9]

$$\partial_t n = -\vec{\nabla}\cdot(n\vec{v}), \tag{17}$$

$$m\partial_t \vec{v} = \vec{\nabla}\left[\frac{\hbar^2}{2m\sqrt{n}}\Delta\sqrt{n} - U_0 n\right] - m\vec{v}(\vec{\nabla}\cdot\vec{v})\,. \tag{18}$$

By taking time derivative of the second equation and linearizing these equations with respect to perturbations of velocity and density, we obtain

$$\partial_t \delta n = -\vec{\nabla}(n\delta\vec{v}) \tag{19}$$

$$m\partial_t^2 \delta\vec{v} = \vec{\nabla}\left[\frac{\hbar^2}{4mn}\Delta\partial_t\delta n + U_0\vec{\nabla}\cdot(n\delta\vec{v})\right]\,. \tag{20}$$

By further simplifications one can obtain an equation on $\delta\vec{v}_{\parallel}$ only, which is a component of the velocity fluctuation along $\vec{k}$. After performing Fourier transformation we get

$$m\omega^2\delta\hat{v}_{\parallel} = \frac{\hbar^2 k^4}{4m}\delta\hat{v}_{\parallel} + U_0 k^2 n\delta\hat{v}_{\parallel}\,, \tag{21}$$

which recovers Eq. (12) for the Bogoliubov spectrum.

Let us estimate the speed of sound in the simulated BEC at the moment of DKC,

$$c_s \sim \frac{\hbar}{m}\sqrt{\frac{3a_s N_0}{R_1 R_2 R_3}} \approx 3\,\mu\mathrm{m/s}\,, \tag{22}$$

where $R_i = (93, 92, 104)\mu$m. One can demonstrate that the cubic anharmonicity exerts a vertical force on the peripheral parts of the cloud similar to the one coming from the harmonic part. Action of this force results to the vertical velocity (with respect to the central part of BEC) $v \sim \tau_\delta F/m = \tau_\delta R_2 \omega_{\delta,2}^2 \approx 1\,\mathrm{mm/s}$, which is 3 orders of magnitude larger than c_s. Based on that, we identify the irregularities in Fig. 4 with shock-waves.

Adiabatic cooling

In this section we present results of an alternative cooling method. We will gradually decrease the frequencies of the trap allowing the cloud expand adiabatically. We simplify the problem by choosing the harmonic approximation for the trap potential. The trap is created by the Z-wire, dimple wire and bias fields. Chip currents are changed in a way that does not move the trap center. We also take into account that precision of the method is limited by stray fields (larger than 2 mG) and choose the length of the cooling procedure accordingly. Trap frequencies are chosen to have the following time-profile [1]:

$$\omega^i(t) = \frac{\omega_T^i + \omega_0^i}{2} + \frac{\omega_T^i - \omega_0^i}{2}\cdot\frac{\tanh\left(5.8[2(t/T)^{1/4} - 1]\right)}{\tanh(5.8)}\,, \tag{23}$$

where T is the duration of the cooling (in our case, $T = 2$ s), ω_T^i is the trap frequency in direction i at the time T, and ω_0^i are initial frequencies of the trap. We depict the frequencies as functions of time in Fig. 5(a), where

$$\omega_0^i = 2\pi\times(1546, 1505, 352)\,\mathrm{Hz}, \tag{24}$$

$$\omega_T^i = 2\pi\times(0.85, 0.82, 0.19)\,\mathrm{Hz}. \tag{25}$$

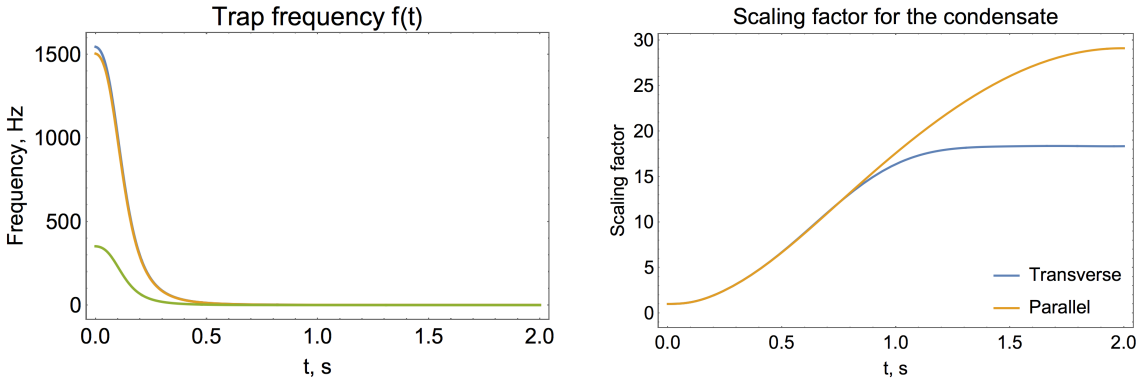

(a) (b)

Figure 5: (a) Frequencies of the trap as a function of time; (b) Change in size of the condensate in the longitudinal and transverse directions (same curve).

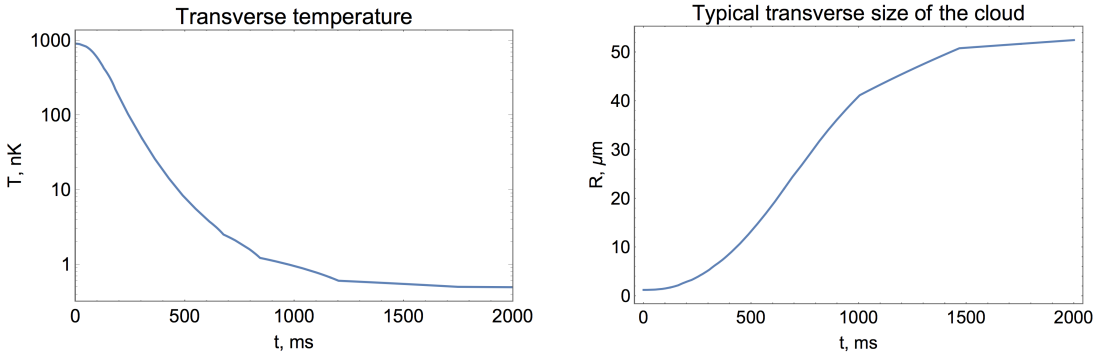

(a) (b)

Figure 6: (a) Transverse temperature of the thermal cloud as a function of time; (b) Transverse temperature of the thermal cloud as a function of time. Fractured line is due to the log-scale interpolation.

We take $N_0 = 10^4$ atoms in the condensate and the same number in the thermal cloud. Simulation for the BEC is done using the scaling ansatz for the Gross-Pitaevskii equation [6]. For the thermal cloud, we assumed no interaction between atoms and applied the Runge-Kutta methods (residual effect of "cooling" due to the rounding error has been taken into account). Results are shown in Figs. 5(b) and 6. The final temperature of the thermal cloud after the adiabatic cooling procedure is approximately 500 pK and the chemical potential of the BEC is $\mu/k_B = 61$ pK, see Eq. (8). This should be considered as the "best-case scenario", since we dismissed the effect of trap anharmonicities and the value of the stray fields can be larger in a real experiment.

References

[1] C.A. Sackett, T.C. Lam, J.C. Stickney, J.H. Burke, Microgravity Sci. Technol. (2017), https://doi.org/10.1007/s12217-017-9584-3

[2] M. P. A. Jones, "Bose-Einstein Condensation on an Atom Chip", PhD thesis, University of Sussex, 2002.

[3] L. D. Landau and E. M. Lifshitz, "Statistical Physics, Part 1"

[4] H. Ammann, N. Christensen, PRL **78** (1997) 3072

[5] S. H. Myrskog, J. K. Fox, H. S. Moon, H. A. Kim, J. B. Kim and A. M. Steinberg, quant-ph/9812031.

[6] Y. Castin and R. Dum, Phys. Rev. Lett. **77**, 5315 (1996).

[7] X. Antoinea, R. Duboscq, Computer Physics Communications 193, (2015), pp. 95-117.

[8] N. N. Bogolyubov, J. Phys. (USSR) **11**, 23 (1947) [Izv. Akad. Nauk Ser. Fiz. **11**, 77 (1947)].

[9] I. Kulikov, M. Zak, Phys. Rev. A **67** (2003), 063605

[10] F. Dalfovo, S. Giorgini, L. P. Pitaevskii and S. Stringari, Rev. Mod. Phys. **71** (1999) 463.